The breakage of nanopore in AAO template

X R Jia, H Wang[1] and Y Zhen

Department of Physics, Capital Normal University, Beijing Key Laboratory of Metamaterials and Devices, Key Laboratory of Terahertz Optoelectronics, Ministry of Education, and Beijing Advanced Innovation Center for Imaging Technology, Beijing, 100048, P.R. China

E-mail: wanghai@cnu.edu.cn

Abstract. In the present work, AAO template is fabricated in oxalic acid solution under a constant voltage by several steps. By the Bernoulli principle, the pressure on the wall of hole increases which lead to the breakage of nanopore as a result of the reducing effective migration rate of Al^{3+}. The quantity of the breakage of nanopore rises with the increase of the concentration of Al^{3+}. Further, nanopore is closed by oxide due to the decrease of effective migration rate of Al^{3+}. Finally, a "nanoflower-like" shape can be observed in experiments.

1. Introduction

AAO films with a hexagonal array structure of mono-disperse nanopore is a template which can be used for the fabrication of nano-materials, such as nanodots [1], nanowires [2] and nanotubes [3], because of the simple preparation technology, the cheap cost, highly ordered pores and with a large aspect ratio.

During the fabrication of AAO template, ions pass through the nanopore array participating electro-chemical reaction. Under the same applied voltage, the density of the ions and its Debye screening length are constant in nanopore. Thus the flow of the ions is incompressible approximately in nanopore. The nanopore array modifies the velocity of ions and the change of velocity may exert a traverse pressure on the wall of nanopore, which leads to the breakage of nanopore array.

In present work, we fabricate AAO template in oxalic acid solution with different Al^{3+} concentration. The concentration of Al^{3+} in solution exerts an influence on the concentration diffusion direction. When the direction of concentration diffusion of Al^{3+} opposites with the directional migration of Al^{3+} under applied electric field, the breakage of nanopores can be easily observed.

2. Experimental

Firstly, high-purity (99.999%) aluminum foil of 0.1mm thickness are degreased in acetone, and then the aluminum foil are washed with deionized water. Secondly, the aluminum foil are electrochemically polished in a 1:4 volume mixture solution of perchloric acid and ethanol to the surface roughness at 10

V for 3 min at 6℃. Thirdly, the AAO films are fabricated by several-step anodization. All the samples are anodized in a 0.3 M oxalic acid solution at 10℃ at 40 V, afterward the formed porous oxide layer are chemically removed in a mixture solution of H_3PO_4 (6wt%) and H_2CrO_4 (1.8wt%) at room temperature. The anodizing time and the time of removing the oxide layer vary with the anodizing step. The anodizing time of from the first step to the sixth step anodic oxidation are 6h, 15min, 5min, 2min, 44s and 16s respectively, and the time of removing the oxide layer formed from the first step to the fifth step are 12h, 2h, 44min, 16min and 6min respectively [4]. Finally, the morphology of the films are observed by scanning electron microscope (SEM) from the Figure 2 to the Figure 6.

The electropolished aluminum are anodized in 0.3M oxalic acid solution at 0℃at 45 V for 6.2h, afterward the formed porous oxide layer are chemically removed in a mixture solution of H_3PO_4 (6wt%) and H_2CrO_4 (1.8wt%) at room temperature for 13h, then the second anodizing step in a 0.3M oxalic acid solution at 0℃ at 45V for 15min, the oxide layer formed in the second steps are removed with a mixture solution of H_3PO_4 (6wt%) and H_2CrO_4 (1.8wt%) at room temperature for 2.3h. The aluminum with hexagonal ordered concave of the second step anodization are anodized in a 0.3M oxalic acid containing saturated Al ion concentration solution at 0℃at 45V for 5min, 8min and 10min respectively. The morphology of the films are observed by scanning electron microscope (SEM) from the Figure 7 to the Figure 9.

3. Discussion

During the process of electrochemical reaction, the velocity of ions are determined by applied voltage and ions concentration gradient. During the preparation of AAO template, the electric field accelerates oxide dissolution to producing Al^{3+}, and $A1^{3+}$ under the drive anodizing electric current and ion concentration gradient current migration from nanopore to the solution [5, 6]. At the interface of nanpores and the solution, in Figure 1, the effective diameter is transforming from pore diameter D_p to interpore distance D_{int}, so the effective cross-sectional area transforms from $S_{pore} = \pi(D_p/2)^2$ to $S_{solution} = \pi(D_{\text{int}}/2)^2$, because the flow of the Al^{3+} is incompressible approximately in nanopore. For incompressible fluid, when the velocity of fluid increases, its pressure decreases. On the contrary, the velocity of fluid decreases, the pressure increase. It is the principle of Bernoulli equation. For the flow of the Al^{3+}, the mass of the Al^{3+} is equal, $S_{pore} * v_{pore} = S_{solution} * v_{solution}$, because of $S_{pore} < S_{solution}$, according to $D_P < D_{\text{int}}$, $v_{pore} > v_{solution}$, that is the velocity of Al^{3+} at the interface of nanopore and solution slow down, in addition the density of the Al^{3+} ρ is constant in nanopore, and the central axis of the Al^{3+} is the center of the pore diameter D_p and the interpore distance D_{int} respectively, so the height of center of gravity h is constant, according to Bernoulli equation $\frac{1}{2}\rho v^2 + \rho gh + P = const$, thus $P_{pore} < P_{solution}$ on account of $v_{pore} > v_{solution}$, that is the pressure enhances at the interface from nanopore to solution.

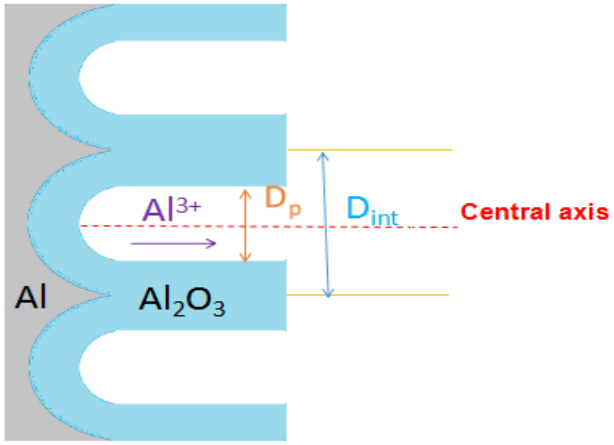

Figure 1. The cross-sectional schematic of the porous alumina film.

During the fabrication of AAO template, the effective velocity of the Al^{3+} are under the influence of the electric field and the ion concentration gradient in the electrolyte. The direction of Al^{3+} migration is from nanopore to solution under the action of the electric field; the electric field accelerates oxide dissolution to producing a number of Al^{3+} spreading into the solution, then the concentration of Al^{3+} in oxalic acid solution increases with time. when the concentration of the Al^{3+} in the pore is larger than in solution, the direction of Al^{3+} migration is from nanopore to solution under the action of ion concentration gradient, the effective velocity of the Al^{3+} is augment on account of the same direction of concentration diffusion of Al^{3+} and the directional migration of Al^{3+} under applied electric field. However when the concentration of the Al^{3+} in the pore is smaller than in solution, the direction of Al^{3+} movement is from solution to nanopore under the action of ion concentration gradient, so the effective velocity of Al^{3+} is decrease on account of the direction of concentration diffusion of Al^{3+} opposite with the directional migration of Al^{3+}.

From the Figure 2 to the Figure 4 show typical SEM images of AAO films after two, three and four-step anodic oxidation. A common feature is a hexagonal array structure of mono-disperse nanopores, while the quantity of the breakage of nanopores is more and more with the increase of oxidation step. We consider the electric field accelerates oxide dissolution to producing a number of Al^{3+} spreading to the solution during the fabrication of AAO template, that result in the concentration of Al^{3+} in oxalic acid solution increase with the increase of oxidation step, and then the effective velocity of Al^{3+} is lower and lower with the increase of oxidation step under the influence of electric field and ion concentration gradient, the effective velocity of the Al^{3+} reducing result in the enhancement of pressure on the wall of nanopore by the Bernoulli principle, so the quantity of the breakage of nanopores is more and more with the increase of oxidation step. Meanwhile at the interface between nanopore and solution, the effective cross-sectional area from $S_{pore} = \pi(D_p/2)^2$ to $S_{solution} = \pi(D_{\text{int}}/2)^2$, the mass of the Al^{3+} is equal, $S_{pore} * v_{pore} = S_{solution} * v_{solution}$. $S_{pore} < S_{solution}$ according to $D_P < D_{\text{int}}$, so $v_{pore} > v_{solution}$. From two-step to four-step anodic oxidation, the concentration of Al^{3+} in oxalic acid solution is not saturated, so the effective velocity of Al^{3+} in the nanopore is not smallest, therefore the

oxide at the surface of nanopores that are fabricated by Al^{3+} from nanopore to solution and the inverse migration oxygen ions is difficult, but Al^{3+} spreading into solution.

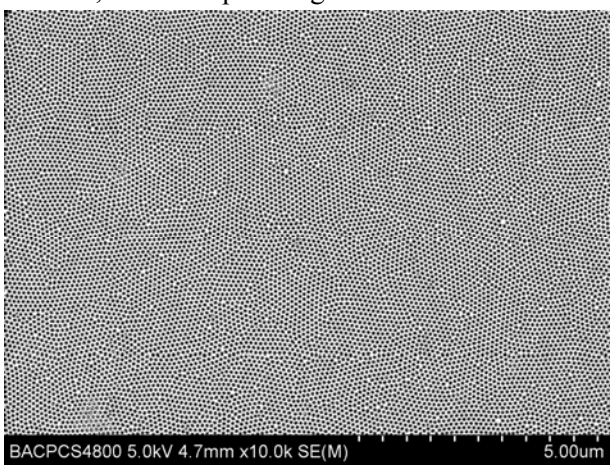

Figure 2.SEM images of AAO film made for 15min by two-step.

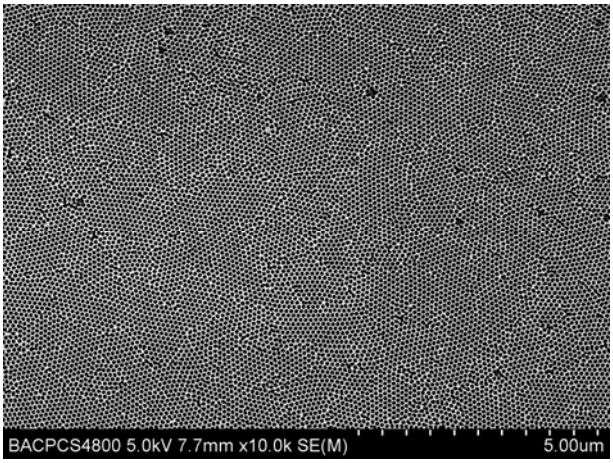

Figure 3.SEM images of AAO film made for 5min by three-step.

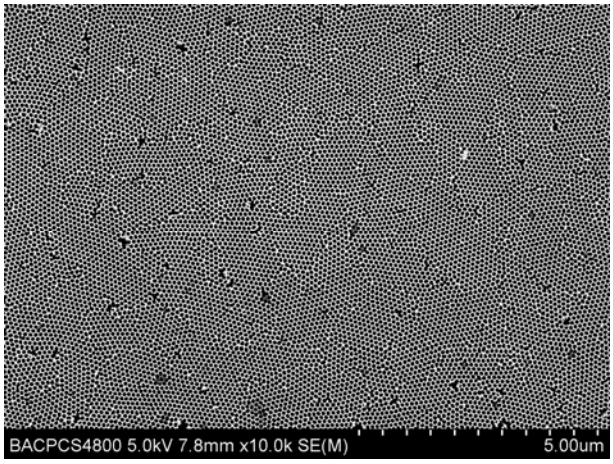

Figure 4. SEM images of AAO film made for 2min by four-step.

The Figure 5 and the Figure 6 show typical SEM images of AAO films by five-step and six-step anodic oxidation, the oxide at the surface of nanopores are fabricated. The Figure 5 show a number of

the "line-like" oxide at the surface of nanopores, although the "line-like" oxide is disorder distribution, its distribution density is almost the same, in addition the "line-like" oxide distribute on the boundary of the domain, and below the "line-like" oxide is mono-disperse nanopore with a hexagonal array structure. We consider the increase of Al^{3+} concentration in oxalic acid solution with the increase of oxidation step, the effective velocity of Al^{3+} is smaller on account of the direction of concentration diffusion of Al^{3+} opposite with the directional migration of Al^{3+} under applied electric field. At the interface of nanopore and solution, the effective cross-sectional area transform from $S_{pore} = \pi(D_p / 2)^2$ to $S_{solution} = \pi(D_{\text{int}} / 2)^2$, the mass of the Al^{3+} is equal, $S_{pore} * v_{pore} = S_{solution} * v_{solution}$. $S_{pore} < S_{solution}$ according to $D_P < D_{\text{int}}$, so $v_{pore} > v_{solution}$. So the effective velocity of the Al^{3+} in the nanopore decrease, therefore the oxide at the surface of nanopores that are fabricated by Al^{3+} from the nanopore to the solution and the inverse migration oxygen ions is easy, especially on the boundary of the domain, it lead to a part of Al^{3+} stacking due to disorder nanopores, so the stacking point of the oxide form "line-like" oxide. The Figure 6 show typical SEM images of AAO films by six-step anodic oxidation, we can observe a large number of the "nanoflower-like" oxide at the surface of nanopores, and the "nanoflower-like" oxide are composed of the middle of "trunk-link" and around "beard-link", also its distribution density is almost the same, and below the "nanoflower-like" oxide is mono-disperse nanopore with a hexagonal array structure. The shape of the oxide in the Figure 6 is larger than in the Figure 5, because the effective velocity of Al^{3+} is lower due to the Al^{3+} higher concentration by six-step anodic oxidation.

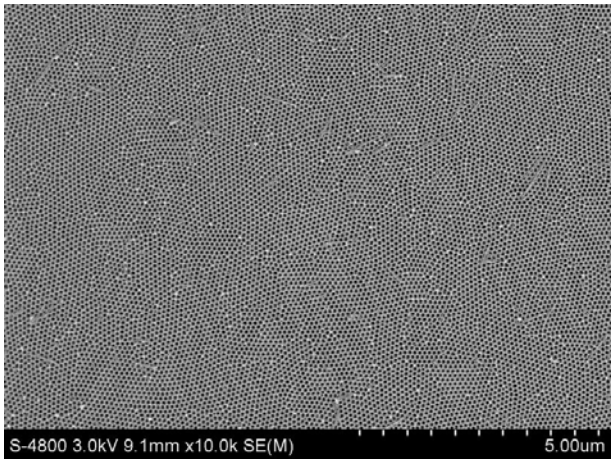

Figure 5. SEM images of AAO film made for 44s by five-step.

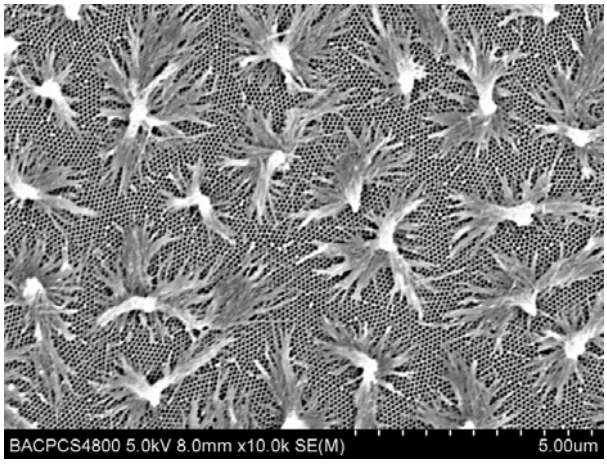

Figure 6. SEM images of AAO film made for16s by six-step.

To prove the conclusion of the oxide at the surface of nanopores that are fabricated by Al^{3+} from the nanopore to the solution and the inverse migration oxygen ions but that are not affected by the oxidation step and time is correct, we change the oxidation parameter. The aluminum with hexagonal ordered concave of the second step anodization are anodized in a 0.3 M oxalic acid solution containing saturated concentration of Al^{3+} at 0℃ at 45 V for 5min by three-step anodic oxidation.

The Figure 7 show typical SEM images of AAO films in oxalic acid solution containing saturated concentrcation of Al^{3+} for 5min by three-step anodic oxidation. We can observe the some of nanopores is closed by oxide at the surface of nanopores, in addition some of the breakage of nanopores in AAO template. When the concentration of Al^{3+} is saturated in the oxalic acid solution, the direction of concentration diffusion of Al^{3+} opposites with the directional migration of Al^{3+} under applied electric field, so the effective velocity of Al^{3+} is the smallest. At the interface of nanopores and solution, the effective cross-sectional area transform from $S_{pore} = \pi(D_p / 2)^2$ to $S_{solution} = \pi(D_{\text{int}} / 2)^2$, the mass of the Al^{3+} is equal, $S_{pore} * v_{pore} = S_{solution} * v_{solution}$, $S_{pore} < S_{solution}$ according to $D_P < D_{\text{int}}$, so $v_{pore} > v_{solution}$. Therefore the effective velocity of Al^{3+} in the nanopore is the lowest, the result in the oxide in surface nanopores are formed by Al^{3+} from the nanopores to the solution and the inverse migration oxygen ions.

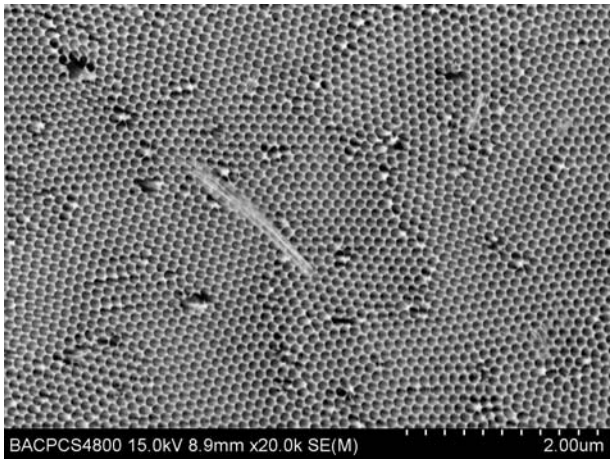

Figure 7. SEM images of AAO film made in saturated Al^{3+} concentration for 5min by three-step.

Figure 8 show typical SEM images of AAO films in oxalic acid solution containing saturated concentration of Al^{3+} for 8min by three-step anodic oxidation.We can observe the breakage of oxide at the surface of nanopores and below the breakage of nanopores is mono-disperse nanopore with a hexagonal array structure. We thought the effective velocity of Al^{3+} reduce due to the Al^{3+} limited in closed nanopores, so the pressure on the wall of nnopore enhance by Bernoulli principle, and then the nanopore break and below the breakage of nanopore is order nanopores. Although the literature are also reported the breakage of nanopore and the reason of the breakage of nanopores is the wall of naopore corroded in acid and alkali solution [7, 8], the theory that the breakage of nanopore the reason why the effective velocity of Al^{3+} reducing lead to the enhancement of pressure on the wall of nanopore is not reported.

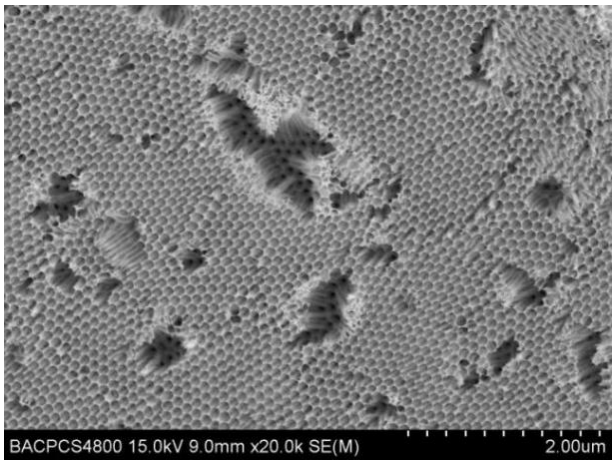

Figure 8. SEM images of AAO film made in saturated Al^{3+} concentration for 8min by three-step.

The Figure 9 show typical SEM images of AAO films in oxalic acid solution containing saturated concentration of Al^{3+} for 10min by three-step anodic oxidation, we can observe a large number of the "nanoflower-like" oxide at the surface of nanopores, and it is composed of the middle of "trunk-like" and around "beard-link", and its distribution density is almost the same, in addition below the "nanoflower-like" oxide is mono-disperse nanopore with a hexagonal array structure. We consider the breakage of nanopore largen when the Al^{3+} in the nanopores pass through the nanopore to solution, finally the alumina of the surface will shrink to form different patterns "nanoflower-like". The middle of

"trunk-link" are originate from the closed oxide at the surface of nanopores shrinking, and the around "beard-link" are originate from the breakage of nanopores.

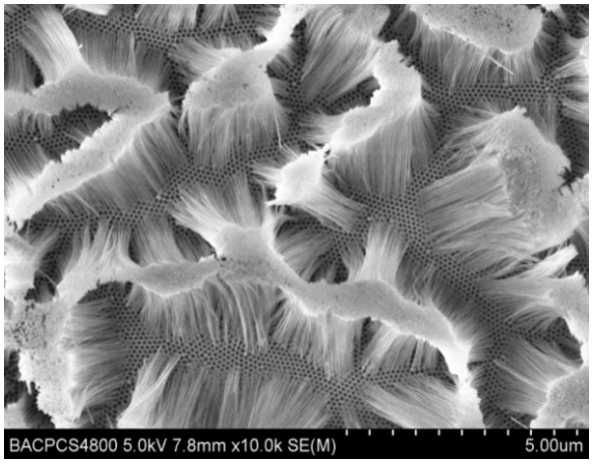

Figure 9. SEM images of AAO film made in saturated Al^{3+} concentration for 10min by three-step.

We can observe the "nanoflower-like" shape are similar from the Figure 6 and the Figure 9. The Figure 9 show typical SEM images of AAO films in oxalic acid solution containing saturated concentration of Al^{3+} under 45V for 10min by three-step anodic oxidation, while the Figure 6 show typical SEM images of AAO films under 40V for 2s by six-step anodic oxidation. Because the oxidation step and time are different, the "nanoflower-like" oxide are not affected of the oxidation step and time. The same parameter is the high concentration of Al^{3+} in oxalic acid solution, so the direction of concentration diffusion of Al^{3+} opposite with the directional migration of Al^{3+} under applied electric field, the result in the effective velocity of Al^{3+} is decrease in the nanopores. Therefore the oxide at the surface of nanopores that are fabricated by Al^{3+} from the nanopore to the solution and the inverse migration oxygen ions is easy. The effective velocity of Al^{3+} reducing lead to the enhancement of pressure on the wall of nanopore by the Bernoulli equation $\frac{1}{2}\rho v^2 + \rho gh + P = const$. Therefore the breakage of nanopores and the "nanoflower-like" oxide are formed.

4. Conclusion

We study the different AAO template fabricated by changing the concentration of Al^{3+} in oxalic acid solution. When the concentration of Al^{3+} is low, the effective velocity of Al^{3+} is large due to the direction of the direction of concentration diffusion of Al^{3+} same with the directional migration of Al^{3+} under applied electric field in the electrolyte. Al^{3+} spreads into the solution easily, which benefits for the order AAO template formation. However, in the case of high Al^{3+} concentration in acid, the direction of the electric field opposites with the ion concentration gradient in the electrolyte. Therefore, the effective velocity of Al^{3+} becomes smaller, which results in the pressure enhancement on the wall of nanopore and leads to the breakage of nanopore finally.

Acknowledgments

This work was financially supported by the National Natural Science Foundation of China (NSFC) with grant No.11274233 and Beijing education committee under grant KM201610028004.

References

[1] Kikuchi N, Okamoto S and Kitakami O 2009 Generation of nanosecond magnetic pulse field for switching experiments on a single Co/Ptnanodot *J Appl Phys.* **105**(07) 506
[2] Yin A, Li J, Jian W, Bennett A and Xu M 2001 Fabrication of highly ordered metallic nanowire arrays by electrodeposition *Appl Phys Lett*. **79**(7) 1039
[3] Kouklin N 2005 Self-assembled network of carbon nanotubes synthesized by chemical vapor deposition in alumina porous template *Appl Phys Lett*. **87**(20) 3105
[4] Zhen Y, Wang H, Jia X, Jiang H and Liu J 2011 The Effect of Multi-Step Anodic Oxidation *Materials Science Forum.* **694** 585
[5] Osullivan J and Wood G 1970 The morphology and mechanism of formation of porous anodic films on aluminum *Proc R Soc London A.* **317** 511
[6] Thompson G 1997 Porous anodic alumina: Fabrication, characterization and applications *Thin Solid Films*. **297**(1-2) 192
[7] Zhang L,Yao S, Zhang W and Wang H 2005 Preparation and Formation Mechanism of Alumina Nanowires *Acta Phys Chim Sin*. **21**(11) 1254
[8] Sun X, Liang J, Zhao J, Ma Q and Xu B 2010 Preparation of alumina nanowires, nanorods, and nanowalls by chemical etching *Appl Phys A*.**98**(10) 263